References

[1]Yang, R., and Wood, B. D., "Experimental Study for Heat and Mass Transfer in Wavy Film Absorption with the Presence of Non-Absorbable Gases," *Chemical Engineering Communications*, Vol. 125, 1993, pp. 77–90.

[2]Ameel, T. A., Habib, H. M., and Wood, B. D., "Effects of a Nonabsorbable Gas on Interfacial Heat and Mass Transfer for the Entrance Region of a Falling Film Absorber," *Journal of Solar Energy Engineering*, Vol. 118, Feb. 1996, pp. 45–49.

[3]Kim, K. J., Berman, N. S., Chau, D. S. C., and Wood, B. D., "Absorption of Water Vapour into Falling Films of Aqueous Lithium Bromide," *International Journal of Refrigeration*, Vol. 18, No. 7, 1995, pp. 486–494.

[4]Chau, D. S. C., Wood, B. D., Berman, N. S., and Kim, K. J., "Solubility of Oxygen in Aqueous Lithium Bromide Using Electrochemical Technique," *International Communication in Heat and Mass Transfer*, Vol. 20, No. 5, 1993, pp. 643–652.

[5]Minkowycz, W. J., and Sparrow, E. M., "Condensation Heat Transfer in the Presence of Noncondensables, Interfacial Resistance, Superheating, Variable Properties, and Diffusion," *International Journal of Heat and Mass Transfer*, Vol. 9, Oct. 1966, pp. 1125–1144.

[6]Sparrow, E. M., Minkowycz, W. J., and Saddy, M., "Forced Convection Condensation in the Presence of Noncondensables and Interfacial Resistance," *International Journal of Heat and Mass Transfer*, Vol. 10, Dec. 1967, pp. 1829–1845.

[7]Othmer, D. F., "Manometer for Determination of Gases in Vapors," *Industrial and Engineering Chemistry, Analytical Edition*, Vol. 1, No. 1, 1929, pp. 46–47.

[8]Ameel, T. A., "Non-Absorbable Gas Effects on Heat and Mass Transfer in Falling Film Absorption," Ph.D. Dissertation, Arizona State Univ., Tempe, AZ, 1991.

[9]Hyland, R. W., and Wexler, A., "Formulations for the Thermodynamic Properties of the Saturated Phases of H_2O from 173.15 K to 473.15 K," Final Rept., American Society of Heating, Refrigerating and Air-Conditioning Engineers, RP 216, Pt. 1, 1980.

[10]Moffat, R. J., "Contributions to the Theory of Single-Sample Uncertainty Analysis," *Journal of Fluids Engineering*, Vol. 104, June 1982, pp. 250–266.

Diffusion Flames in Cylindrical Packed Beds

K. Kamiuto* and T. Ogawa†
Oita University, Oita 870-11, Japan

Introduction

FUNDAMENTAL research[1] on the combustion in porous media is of great practical importance in connection with developments of porous radiant burners and regenerative-type combustors, which yield lean combustion and lower NO_x emissions; several theoretical and experimental studies[2–5] have been performed on this subject. Almost all of these earlier studies, however, were concerned with the premixed combustion in porous media, and little is known about diffusion combustion in porous media.

The purpose of this Note is to remedy this deficiency. First, the flame sheet model,[6,7] taking into account the effect of mass dispersion within a packed bed, is proposed, and then, based on this model, the characteristic features of the flame heights of diffusion flames in packed beds are discussed. In addition, experiments for methane–oxygen diffusion combustion in a cylindrical packed bed of alumina spheres are made to observe actual flame shapes in the packed bed and to address the predictability of the proposed flame sheet model for diffusion flames in packed beds.

Received Sept. 25, 1996; revision received March 31, 1997; accepted for publication April 9, 1997.

*Professor, High-Temperature Heat Transfer Laboratory, Department of Production Systems Engineering. Member AIAA.

†Student, Department of Production Systems Engineering.

Theoretical Model

We assume that 1) a combustion chamber consists of a cylindrical tube randomly packed with uniform, noncatalytic spherical particles; 2) the porosity distribution throughout the combustion chamber is uniform and the mean porosity is 0.39; 3) fuel is injected into the combustion chamber through a tube of radius r_f, concentrically located inside a large tube of radius r_0 through which an oxidant flow occurs; 4) oxidization of the fuel occurs in a thin sheet of space, when the oxidant and the fuel are in stoichiometric proportions; 5) diffusion alone plays a decisive role in determining the shape of the flame, and the diffusion coefficient is independent of temperature and composition; and 6) velocities of the fuel and oxidant flows are equal and constant axially and radially within the combustion chamber.

Under the foregoing assumptions, the conservation equations of chemical species are reduced to the following form:

$$u\frac{\partial\left(Y_f-\dfrac{Y_o}{i}\right)}{\partial x}=\frac{(D_e+D_d)}{r}\frac{\partial}{\partial r}\left[r\frac{\partial\left(Y_f-\dfrac{Y_o}{i}\right)}{\partial r}\right] \tag{1}$$

where x and r are the axial and radial coordinates, Y_f and Y_o, respectively, denoting the mass fractions of fuel and oxidant; u is the Darcy velocity of the fuel and oxidant. D_e and D_d represent the effective diffusivity and the mass dispersion coefficient, respectively, and these quantities are given as follows[8]:

$$D_e = \phi D_m \tag{2}$$

$$D_d = \gamma_m d_p u \tag{3}$$

$$\gamma_m = 0.3519(1-\phi)^{2.3819} \tag{4}$$

Here, ϕ is the mean porosity of a packed bed, D_m is the molecular diffusion coefficient, γ_m is the lateral mixing function for mass dispersion, and d_p is the mean particle diameter. The boundary conditions to Eq. (1) are

$$\begin{aligned} &x=0, && 0\le r\le r_f:\ Y_f-\frac{Y_o}{i}=Y_{fi}\\ & && r_f< r\le r_0:\ Y_f-\frac{Y_o}{i}=-\frac{Y_{oi}}{i}\\ &x\ge 0,\quad r=0, && r=r_0:\ \frac{\partial\left(Y_f-\dfrac{Y_o}{i}\right)}{\partial r}=0 \end{aligned} \tag{5}$$

where Y_{fi} and Y_{oi} denote the mass fractions of the fuel and the oxidant at the inlet of the combustion chamber, respectively, and i is a quantity representing how much oxygen stoichiometrically combines with fuel. To rewrite the governing equation in dimensionless form, the following quantities are introduced:

$$\begin{gathered} K=(D_e+D_d)/ur_0=2(\phi/ReSc+\gamma_m/2\Gamma)\\ Re=2ur_0/\nu,\qquad Sc=\nu/D_m,\qquad \Gamma=r_0/d_p\\ \eta=r/r_0,\qquad \eta_f=r_f/r_0,\qquad \xi=x/r_0 \end{gathered} \tag{6}$$

where ν is the kinematic viscosity of a gas and is constant, irrespective of the kind of chemical species. The dimensionless total lateral diffusion coefficient K takes a minimum at $\phi^*[=1 - 1.8763(\Gamma/ReSc)^{0.7236}]$, which is obtained by solving $\partial K/\partial\phi = 0$: for the molecular diffusion dominant case, i.e., $\phi > \phi^*$, K increases with ϕ; whereas, for the mass dispersion dominant case, i.e., $\phi < \phi^*$, K increases with a decrease in ϕ. As a result, we obtain

$$\frac{\partial\left(Y_f - \frac{Y_o}{i}\right)}{\partial\xi} = \frac{K}{\eta}\frac{\partial}{\partial\eta}\left[\eta\frac{\partial\left(Y_f - \frac{Y_o}{i}\right)}{\partial\eta}\right] \tag{7}$$

$$\begin{aligned} \xi = 0, \quad 0 \le \eta \le \eta_f&: Y_f - \frac{Y_o}{i} = Y_{\mathrm{fi}} \\ \eta_f < \eta \le 1&: Y_f - \frac{Y_o}{i} = -\frac{Y_{\mathrm{oi}}}{i} \\ \xi \ge 0, \quad \eta = 0, 1&: \frac{\partial\left(Y_f - \frac{Y_o}{i}\right)}{\partial\eta} = 0 \end{aligned} \tag{8}$$

Because K is assumed to be constant, Eq. (7) can be solved analytically to yield the following:

$$Y_f - \frac{Y_o}{i} = \left(Y_{\mathrm{fi}} + \frac{Y_{\mathrm{oi}}}{i}\right)\eta_f^2 - \frac{Y_{\mathrm{oi}}}{i} + 2\eta_f\left(Y_{\mathrm{fi}} + \frac{Y_{\mathrm{oi}}}{i}\right) \times \sum_{n=1}^{\infty}\frac{J_1(P_n\eta_f)J_0(P_n\eta)}{P_nJ_0^2(P_n)}\exp(-KP_n^2\xi) \tag{9}$$

Here, P_n denotes the nth positive zeros of the Bessel function of the first order, $J_1(x)$. The dimensionless flame location denoted by (ξ_c, η_c) is determined by the following equation, which can be obtained by letting $Y_f - Y_o/i = 0$ in Eq. (9):

$$\sum_{n=1}^{\infty}\frac{J_1(P_n\eta_f)J_0(P_n\eta_c)}{P_nJ_0^2(P_n)}\exp(-KP_n^2\xi_c) = E_f \tag{10}$$

$$E_f = \left[\frac{Y_{\mathrm{oi}}}{i} - \left(Y_{\mathrm{fi}} + \frac{Y_{\mathrm{oi}}}{i}\right)\eta_f^2\right]\Bigg/\left[2\eta_f\left(Y_{\mathrm{fi}} + \frac{Y_{\mathrm{oi}}}{i}\right)\right] \tag{11}$$

Setting $\eta_c = 0$ for $E_f > 0$, and $\eta_c = 1$ for $E_f < 0$ in Eq. (10), gives the flame height ξ_c^*. Because the flame height is generally large enough and, in addition, P_n increase rapidly with n, the exponential term in Eq. (10) decays quite rapidly; therefore, retaining only the first term in the summation series gives a good estimate to ξ_c^*:

$$\xi_c^* = -\left(\ell n[E_fP_1J_0^2(P_1)/[J_1(P_1\eta_f)J_0(P_1\eta_c)]]\right) / [2P_1^2(\phi/ReSc + \gamma_m/2\Gamma)] \tag{12}$$

where $P_1 = 3.83171$.

This analytical expression for ξ_c^* indicates that the flame height elongates with Re and/or Γ, and shrinks with an increase in ϕ as long as ϕ is greater than ϕ^*. These results are caused by the fact that the overall lateral diffusion coefficient of chemical species K becomes small with an increase in Γ and rises with ϕ for $\phi > \phi^*$, and that the residence time of chemical species within a combustion chamber diminishes as Re becomes large. It is worth noting, however, that when $\phi < \phi^*$, the flame height increases with ϕ, because K decreases with an increase in ϕ. Moreover, when a combustion chamber is not filled with solid spheres, i.e., $\phi = 1$, ξ_c^* becomes infinite as $ReSc \to \infty$; whereas, in a packed-bed combustor, there exists a certain limiting value of ξ_c^*, even when $ReSc \to \infty$.

Experiments

To examine the predictability of the previously mentioned theoretical model for the flame shape in a porous medium, experiments for methane–oxygen diffusion combustion in a packed bed were made. The gas burner utilized was of the double concentric type, consisting of a 70-mm-i.d. brass tube with a 14-mm-i.d. porcelain tube in the middle. The methane gas entered through the porcelain tube, and the oxygen entered through the annulus between the brass and porcelain tubes. Metallic mesh screens were settled at 1 cm upstream from the exit of the burner to support the packed spheres. A cylindrical combustion chamber was attached to the top of the burner. The wall of the combustion chamber was made of a transparent silica glass tube with an i.d. of 70 mm. Two kinds of alumina sphere (93.0 wt %, etc.) with different mean diameters were used as a packing material: $d_p = 2.02$ mm ($\Gamma = 17.3$) and 3.18 mm ($\Gamma = 11.0$). Experiments were made in accordance with the following procedures. First, make the combustion chamber empty and then feed methane and oxygen gases at a prescribed velocity. After ignition, pour an amount of alumina spheres randomly to form a packed bed with a constant height. Take photographs of the surface of the combustion chamber from above and then change the height by adding the packed spheres. The mean porosity of the packed bed was found to be about 0.39, irrespective of the bed height. The bed height, defined by the distance from the exit of the burner, was varied from 0 to 15 cm by a step of 0.5 cm. In addition, gas velocity was varied as follows: $u = 3.24 \times 10^{-2}$ (m/s) ($Re = 64.9$), 4.42×10^{-2} (m/s) ($Re = 88.4$), and 5.89×10^{-2} (m/s) ($Re = 117.9$). Flame shapes were reconstructed from photographs of the upper surface of the packed-bed combustor because, as seen from Fig. 1, an almost annular, luminous zone was formed on the upper surface of the combustor and was considered to indicate a location of the flame surface. However, it was hard to infer a flame shape near the top of the flame by this method because, as the height of the packed bed increased, luminous zones became broad and dull. For this reason, the upper part of a flame profile could not be experimentally reconstructed.

To examine whether the flame position at a given height remains the same after the bed height has been changed, we measured a radial temperature profile at a given height by changing the bed thickness. As a result, it was found that the radial temperature profile is scarcely affected by the bed height, and the radial position of a maximum temperature corresponds well to the location of the flame surface reconstructed from the photographs of the upper surface of the bed.

Photographs of side views of flames in the empty combustor were also taken and analyzed, but they were not shown here.

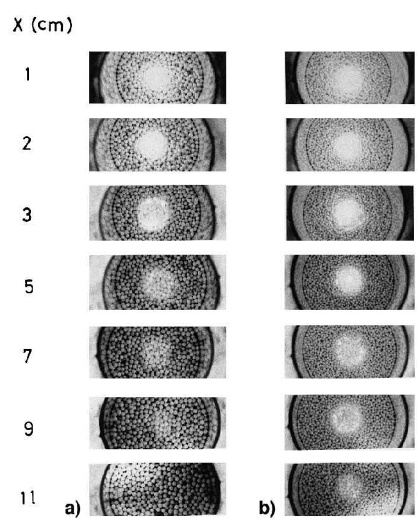

Fig. 1 Photographs of the upper surface of the packed-bed combustor in diffusion combustion: a) $\Gamma = 11.0$ and $Re = 117.9$, and b) $\Gamma = 17.3$ and $Re = 117.9$.

Discussion

Theoretical computations for methane–oxygen diffusion flames (i = 3.989) were performed by solving Eq. (10), utilizing a bisection method with an absolute error less than 2^{-25}. The value of D_m required was assumed to be 4.923×10^{-5} (m^2/s), which was taken from Ref. 6. This value corresponds to the molecular diffusion coefficient for the system CH_4–O_2 at 470 K and 1 bar. However, it should be stressed that a value of K does not depend on $ReSc$, including D_m, when $ReSc \rightarrow \infty$.

Comparisons between experimentally determined flame shapes and predicted ones are made in Figs. 2–4. Figure 2 is concerned with flames in the empty cylindrical combustor; whereas Figs. 3 and 4 compare flames in the packed-bed combustor. As seen from Figs. 2–4, agreement between theory and experiment is satisfactory within an accuracy of the measurements, which was estimated to be ±4%; the proposed theoretical model predicts the effects of Re, Γ, and ϕ on the flame shape. The discrepancies between theory and experiment in Figs. 3 and 4 are attributable to the effect of thermal radiation, which is disregarded in the present analyses.

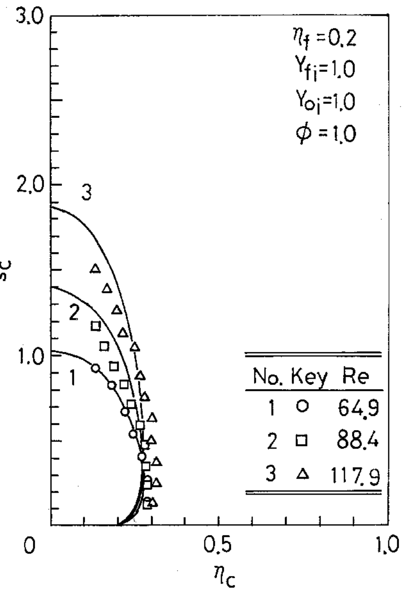

Fig. 2 Comparison between theory and experiment for profiles of methane–oxygen diffusion flames in the empty cylindrical combustor.

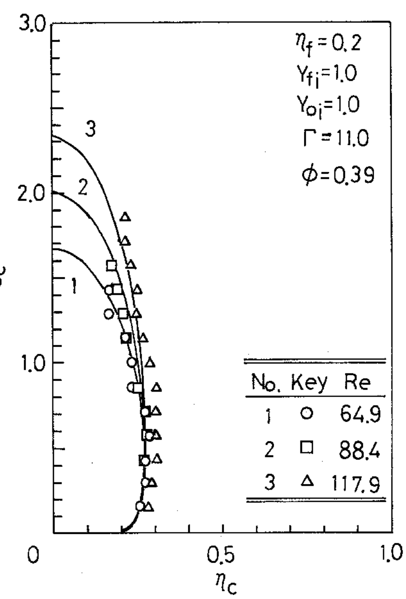

Fig. 3 Comparison between theory and experiment for profiles of methane–oxygen diffusion flames in the cylindrical packed-bed combustor with Γ = 11.0.

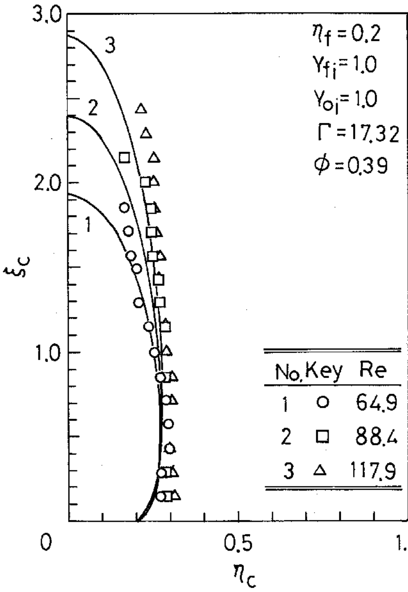

Fig. 4 Comparison between theory and experiment for profiles of methane–oxygen diffusion flames in the cylindrical packed-bed combustor with Γ = 17.3.

Conclusions

The major conclusions that can be drawn from the present study are summarized as follows:

1) The flame shape in a packed bed elongates with Re and/or Γ, and shrinks with an increase in ϕ as long as ϕ is greater than $\phi^*[=1 - 1.8763(\Gamma/ReSc)^{0.7236}]$.

2) The proposed flame sheet model predicts the observed effects of Re, Γ, and ϕ on the flame shape in a packed bed.

3) The proposed flame sheet model predicts that the flame height in a packed bed is finite, even when $ReSc \rightarrow \infty$.

Acknowledgment

The authors express their sincere gratitude to R. Echigo, of the Tokyo Institute of Technology, who encouraged the authors to perform this study.

References

[1]Penner, S. S., and Berland, A. L., "Fundamental Combustion Research in Support of Industrial Applications," *Energy—The International Journal*, Vol. 20, No. 4, 1995, pp. 311–324.

[2]Echigo, R., Yoshizawa, Y., and Hanamura, K., "Analytical and Experimental Studies on Radiative Propagation in Porous Media with Internal Heat Generation," *Heat Transfer 1986*, Hemisphere, Washington, DC, 1986, pp. 827–832.

[3]Chen, Y.-K., Mattheus, R. D., and Howell, J. R., "The Effect of Radiation on the Structure of Premixed Flame Within a Highly Porous Inert Media," American Society of Mechanical Engineers, HTD-Vol. 81, New York, 1987, pp. 35–42.

[4]Tong, T. W., and Sathe, S. B., "Heat Transfer Characteristics of Porous Radiant Burners," *Journal of Heat Transfer*, Vol. 113, May 1991, pp. 423–428.

[5]Hanamura, K., Echigo, R., and Zhdanok, S. A., "Super Adiabatic Combustion in Porous Media," *International Journal of Heat and Mass Transfer*, Vol. 36, No. 12, 1993, pp. 3201–3209.

[6]Burke, S. P., and Schumann, T. E. W., "Diffusion Flames," *Industrial and Engineering Chemistry*, Vol. 20, No. 10, 1928, pp. 998–1005.

[7]Kanury, A. M., *Introduction to Combustion Phenomena*, Gordon and Breach, New York, 1994, pp. 259–265.

[8]Kamiuto, K., and Saitoh, S., "Simultaneous Heat and Mass Transfer in Packed Bed Catalytic Reactors," *Journal of Thermophysics and Heat Transfer*, Vol. 9, No. 3, 1995, pp. 524–530.